Comparison of Optical Coherence Tomography and Ultrasound Biomicroscopy for Detection of Narrow Anterior Chamber Angles

Sunita Radhakrishnan, MD; Jason Goldsmith, MD; David Huang, MD; Volker Westphal, PhD; David K. Dueker, MD; Andrew M. Rollins, PhD; Joseph A. Izatt, PhD; Scott D. Smith, MD, MPH

Objective: To assess the accuracy of classification of narrow anterior chamber (AC) angles using quantitative imaging by optical coherence tomography (OCT) and ultrasound biomicroscopy (UBM).

Design: Observational comparative study.

Methods: A high-speed (4000 axial scans/s) anterior segment OCT prototype was developed using a 1.3-μm light source. Seventeen normal subjects (17 eyes) and 7 subjects (14 eyes) with narrow angle glaucoma were enrolled. All subjects underwent gonioscopy, OCT, and UBM. Quantitative AC angle parameters (angle opening distance, angle recess area, and the trabecular-iris space area [a new parameter we have defined]) were measured from OCT and UBM images using proprietary processing software.

Main Outcome Measures: Specificity and sensitivity in identifying narrow angles with image-derived AC angle parameters.

Results: Eight of 31 eyes were classified as having narrow angles (Shaffer grade ≤1 in all quadrants). The AC angle parameters measured by both OCT and UBM had similar mean values, reproducibility, and sensitivity-specificity profiles. Both OCT and UBM showed excellent performance in identifying eyes with narrow angles. Areas under the receiver operating characteristic curves for these parameters were all in the range of 0.96 to 0.98.

Conclusions: Optical coherence tomography was similar to UBM in quantitative AC angle measurement and detection of narrow angles. In addition, it was easier to use and did not require contact with the eye. Optical coherence tomography is a promising method for screening individuals at risk for narrow angle glaucoma.

Arch Ophthalmol. 2005;123:1053-1059

Author Affiliations: Cole Eye Institute, Cleveland Clinic Foundation (Drs Radhakrishnan, Goldsmith, Huang, Dueker, and Smith), and Departments of Medicine (Drs Radhakrishnan, Westphal, and Rollins) and Biomedical Engineering (Drs Westphal and Izatt), Case Western Reserve University, Cleveland, Ohio. Dr Izatt is now with the Department of Biomedical Engineering, Duke University, Durham, NC.

Financial Disclosure: Dr Huang has provided research support to Carl Zeiss Meditec Inc, Dublin, Calif, and has received a patent royalty for optical coherence tomography.

PRIMARY ANGLE CLOSURE GLAUCOMA (PACG) is highly prevalent in certain regions of the world.[1-4] Although prospective data are currently lacking, it is widely believed that treating anatomically narrow angles with a laser periphery iridotomy may prevent development of angle closure. Therefore, early detection of anatomically narrow angles is important.

Currently, gonioscopy is the clinical standard for assessing the risk of PACG. However, it is a subjective technique and there are no uniform gonioscopic criteria for identifying angles that require treatment.[5,6] Cross-sectional imaging of the anterior chamber (AC) angle can provide quantitative data and may prove to be less subjective than gonioscopy. Ultrasound biomicroscopy (UBM)[7] has been used in identifying anatomical characteristics of eyes with narrow AC angles.[8-11] However, UBM requires immersion of the eye in fluid and is therefore time-consuming and inconvenient to perform in the routine clinical setting. Optical coherence tomography (OCT)[12] is an alternative cross-sectional imaging modality that is light-based and does not require contact with the eye. In this study, we have used OCT to quantify the AC angle and to assess its potential in the detection of eyes at risk of angle closure. To our knowledge, this is the first time OCT has been described for this application.

Optical coherence tomography is analogous to ultrasonography in that a probe beam is directed onto biological tissue, and the reflections returning from the sample are analyzed to obtain depth information. In ultrasonography, the depth of tissue structures is determined by directly measuring the time delay of the returning ultrasound signal. Since light travels much more quickly than sound, the time delay of the returning light reflection in OCT is determined indirectly by the method of low-coherence interferometry.

Ophthalmic OCT was initially developed for posterior segment imaging[13,14] and utilized 0.8-µm wavelength light sources. Anterior segment imaging at this wavelength has been reported by several investigators who used either prototype OCT systems[15,16] or the commercially available retinal OCT scanner (Carl Zeiss Meditec Inc, Dublin, Calif).[17-21] The majority of these studies focused on corneal imaging. With regard to AC angle imaging, however, these OCT systems are suboptimal for tissue delineation because 0.8-µm light cannot penetrate the sclera, thereby preventing visualization of the underlying angle structures. In contrast, OCT at 1.3-µm wavelength of light is better suited for AC angle imaging due to 2 significant properties. First, the amount of scattering in tissue is lower at this wavelength.[22] This enables increased penetration through scattering ocular structures such as the sclera and the iris so that AC angle morphology is visualized with more detail. Second, 1.3-µm wavelength of light is strongly absorbed by water in the ocular media and, therefore, only 10% of the light incident on the cornea reaches the retina.[23] This improved retinal protection allows for the use of higher-power illumination that, in turn, enables high-speed imaging.

Hoerauf et al[24] have reported transscleral OCT imaging in enucleated pig eyes using a 1.3-µm light source. Though this prototype allowed for better visualization of the angle region, it resembled the 0.8-µm OCT systems in that the image acquisition rate was slow (1-2 seconds per image). A high-speed imaging system is desirable for several reasons. It eliminates motion artifacts, reduces examination time, allows for rapid survey of relatively large areas, and enables imaging of dynamic ocular events.

We have developed an anterior segment OCT system[25] with the high speed required for imaging in near real time. The scanning speed is 40 times faster than previous anterior segment OCT systems, and the use of a 1.3-µm light source permits detailed visualization of the AC angle region. These system features enable quantitative AC angle evaluation with OCT. In this pilot study, we have compared UBM and OCT for imaging of the anterior segment in a small group of subjects, with a focus on quantitative characterization of the AC angle. We analyzed quantitative angle parameters to determine the feasibility of using OCT for detection of narrow angles as defined by the gonioscopic criteria used at our institution.

METHODS

The institutional review boards of the University Hospitals of Cleveland and the Cleveland Clinic Foundation approved this prospective observational study. To obtain the complete range of AC angle width, we recruited 17 normal volunteers (17 eyes) from the Division of Ophthalmology at the Cleveland Clinic Foundation as well as 7 subjects (14 eyes) with narrow angles from the Glaucoma Department of the Cleveland Clinic Foundation. After obtaining informed consent, all of the subjects underwent OCT, UBM, and gonioscopy; OCT imaging was done prior to any contact procedure. Both OCT and UBM were performed under uniform conditions of dim illumination that was standardized using a light meter. The room illumination was adjusted such that similar light meter readings were obtained at the eye level of a test subject positioned for scanning at each of the 2 instruments; this illumination level was then maintained for all of the subjects in the study. Gonioscopy was also performed under dim ambient light; however, the light intensity was not standardized.

Optical coherence tomography was performed using a prototype that has been described previously.[25] In brief, this system used a semiconductor optical amplifier light source capable of emitting 22 mW of low-coherence light with a central wavelength of 1.3 µm and a spectral bandwidth of 68 nm full-width at half-maximum. The optical power incident on the eye was 4.9 mW, which is well within the American National Standards Institute maximum permissible exposure limit of 15.4 mW for this wavelength.[26] The scanning speed was 4000 axial scans per second and each image frame had 500 axial scans per image, giving an image acquisition rate of 8 frames per second. The lateral resolution was 15 µm and the axial resolution was 8 µm. Additional features in the system used for this study were that the OCT probe was mounted on a slitlamp base, the image display was in gray scale, and the scan depth was selectable between 4 mm and 7 mm in air.

Optical coherence tomographic imaging of the AC angle was performed with the subject in the sitting position, and the image size was 3.77 mm wide and 4.00 mm deep. Ultrasound biomicroscopy was performed with a 50-MHz probe (Ultrasound Biomicroscope System Model 840; Humphrey Instruments Inc, San Leandro, Calif). Subjects were examined in the supine position with the eye immersed in saline solution using a 22-mm or 24-mm eyecup. The UBM image size was 5.00 mm wide and 5.00 mm deep. With both techniques, 3 images each of the central cornea and the central AC were recorded in primary gaze and 3 images each of the temporal and nasal AC angles were recorded in lateral gaze. These quadrants were selected so that no contact whatsoever was required with the patient to acquire the OCT images.

MEASUREMENT OF OCT AND UBM IMAGES

Optical coherence tomographic images were processed offline using custom software[27] that corrected image distortions arising from 2 sources: first, the fan-shaped scanning geometry of the OCT beam, and second, the effects of refraction at the cornea-air interface. Calibration and geometric transformation of the image in the software corrected the former, and the effects of refraction were corrected by segmenting the anterior and posterior corneal surfaces, then using a custom computer algorithm to determine the true paths of the light rays propagating in the eye. Following this image processing, the OCT images were measured with quantitative tools that were also provided in the custom software.

The stored UBM images were measured using the same custom software. Image processing was not performed prior to measurement because, unlike OCT, the ultrasound beam emerging from the UBM probe had a linear scanning geometry and did not cause distortions in the rectilinearly displayed image.

The anterior segment parameters that were measured were as follows. For each parameter, the mean of 3 measurements obtained from each eye was used as the final value.

1. Angle opening distance at 500 µm (AOD 500; **Figure 1**): On both OCT and UBM images, the AOD 500 was measured as described by Pavlin et al.[28] The scleral spur was first identified and a point was marked 500 µm anterior to it. From this point, a line was drawn perpendicular to the plane of the trabecular meshwork to the opposing iris and the distance between these last 2 points was defined as the AOD 500.

2. Angle recess area at 500 µm and 750 µm (ARA 500 [Figure 1] and ARA 750, respectively): On both OCT and UBM images, the ARA was measured as described by Ishikawa et al.[29]

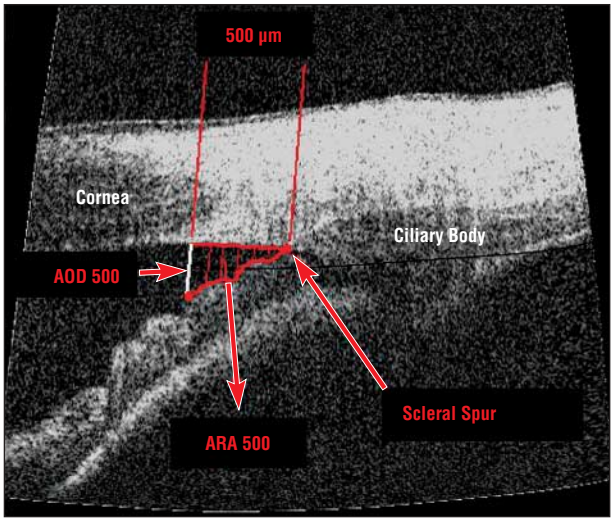

Figure 1. Angle opening distance at 500 µm (AOD 500) and angle recess area at 500 µm (ARA 500) depicted on an optical coherence tomographic image of a lightly pigmented eye. Note that the ARA follows the iris contour.

The defining boundaries of this triangular area are the AOD 500 or AOD 750 (the base), the angle recess (the apex), and the iris surface and inner corneoscleral wall (sides of the triangle). The ARA is, theoretically, a better measurement parameter than the AOD because it takes into account the whole contour of the iris surface rather than measuring at a single point on the iris as is the case with the AOD.

3. Trabecular-iris space area at 500 µm and 750 µm (TISA 500 [**Figure 2**] and TISA 750, respectively): We propose this new parameter for quantitative measurement of the AC angle. The defining boundaries for this trapezoidal area are as follows: anteriorly, the AOD 500 or AOD 750; posteriorly, a line drawn from the scleral spur perpendicular to the plane of the inner scleral wall to the opposing iris; superiorly, the inner corneoscleral wall; and inferiorly, the iris surface. The TISA 500 and the TISA 750 were measured on both UBM and OCT images. We feel that this parameter represents the actual filtering area more accurately when compared with the ARA because the TISA excludes the nonfiltering region behind the scleral spur.

4. Trabecular-iris contact length (TICL; **Figure 3**): We propose this new parameter to describe an anatomically closed angle. The TICL is defined as the linear distance of iris contact with the corneoscleral surface beginning at the scleral spur and extending anteriorly in an anatomically apposed or synechially closed angle.

Gonioscopy was performed in each subject by 1 of 2 independent glaucoma specialists (D.K.D. and S.D.S.) using a Zeiss 4-mirror gonioscopy lens, and grading was recorded for each of the 4 AC angle quadrants according to the following scale: grade 4, wide open angle with a flat or concave iris surface and the scleral spur visible without positioning the eye toward the gonioscopy mirror; grade 3, wide open angle with a slightly convex iris surface and the scleral spur visible without positioning the eye toward the gonioscopy mirror; grade 2, open angle with a convex iris surface and the scleral spur visible without positioning the eye toward the gonioscopy mirror; grade 1, narrow angle with a convex iris surface and the scleral spur visible only with the positioning of the eye toward the gonioscopy mirror; and grade 0, extremely narrow or closed angle and the scleral spur not visible even with positioning the eye toward the gonioscopy mirror.

A narrow angle was defined as Shaffer grade 1 or lower in all quadrants. Indentation gonioscopy was not performed because the focus of this study was to measure angle width and not to differentiate appositional vs synechial closure; the presence or absence of peripheral anterior synechiae would not have altered the study outcome.

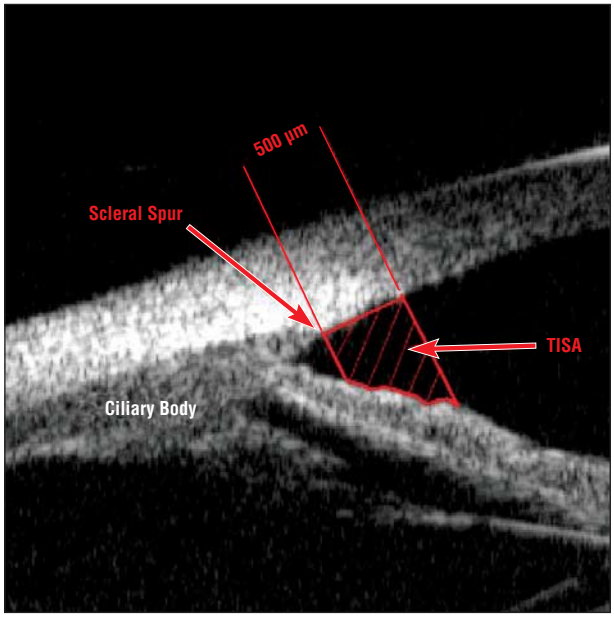

Figure 2. Trabecular-iris space area (TISA) at 500 µm measured on an ultrasound biomicroscopic image of a subject with a deep angle recess. Note that the area behind the scleral spur is not included in the TISA.

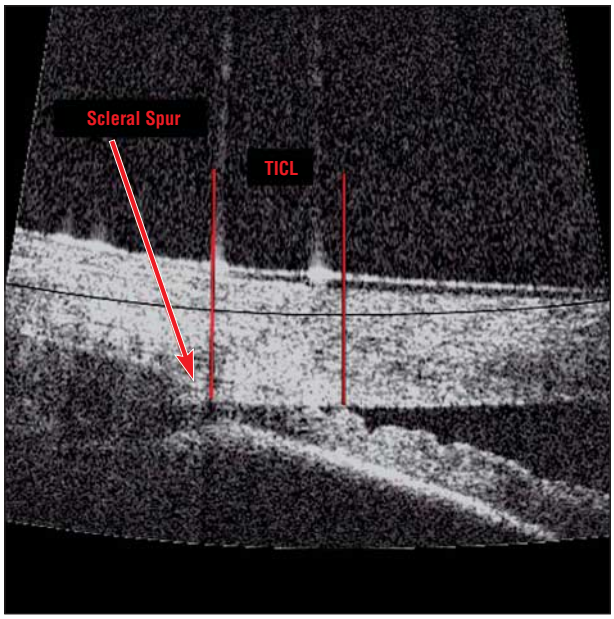

Figure 3. Trabecular-iris contact length (TICL) depicted on an optical coherence tomographic image of a subject with narrow angles on gonioscopy.

STATISTICAL METHODS

Mean values of parameters measured by UBM and OCT were compared using the paired *t* test. The discriminative ability of the measured parameters in identifying narrow angles was determined by calculating sensitivity and specificity based on several alternative cutoff values and by the area under the receiver operating characteristic curve (AUC).

RESULTS

Thirty-one eyes of 24 subjects were included in the study. The subjects' mean age was 42.9 years. Fifteen subjects (62.5%) were women. The majority of subjects were white (n=14, 58.3%), with smaller numbers of subjects of other races (African American, n=14, 12.5%; Asian, n=4, 16.7%; East Indian, n=2, 8.3%; Hispanic, n=1, 4.2%). Eight eyes (25.8%) were classified on gonioscopy as having narrow angles, defined as grade 1 or lower in all quadrants (**Table 1**).

Figure 4 shows UBM and OCT images of the AC angle. Optical coherence tomographic images showed sharper definition of the scleral spur when compared with UBM images. Optical coherence tomography, however, could not image the entire ciliary body well due to attenuation of light by the overlying sclera.

Mean values of the angle parameters measured by UBM and OCT were very similar (**Table 2**). However, small but statistically significant differences were observed in some parameters. Generally, the value of the parameter was smaller when measured by UBM. Repeatability as assessed by the pooled standard deviation of the repeated measures was not significantly different between the 2 imaging modalities.

Each of the measured parameters performed well in distinguishing narrow angles (**Table 3**). Alternative definitions of a positive test result were evaluated for each parameter to identify optimum values that provided the best possible mix of sensitivity and specificity. The average of 2 measurements from the nasal and temporal quadrants in each eye was used. No significant difference was found between OCT and UBM parameters. The high level of efficiency in discriminating narrow angles from open angles is illustrated by the receiver operating characteristic curve of the TISA measured at 750 µm by OCT (**Figure 5**). The AUC of 0.96 (95% confidence interval, 0.90-1.00) shows that, based on the present sample, this parameter has nearly perfect discriminative ability. **Table 4** lists the AUC for all of the parameters measured in this study.

Another parameter, the TICL, was also evaluated. This parameter represents the measured length of contact between the iris and angle structures anterior to the scleral spur. Subjects were classified according to the presence or absence of identifiable trabecular-iris contact (ie, TICL >0). In 16 (12.9%) of 124 images acquired by UBM, nonzero values of TICL were identified. These 16 positive values of TICL occurred in at least 1 image in 7 (87.5%) of 8 subjects with a gonioscopic grade of 1 or lower, and 5 (21.7%) of 23 subjects with a grade of 2 or higher. In 11 (8.9%) of 124 images acquired by OCT, nonzero values of TICL were identified. These positive values occurred in 5 (62.5%) of 8 subjects with a gonioscopic grade of 1 or lower and in no subjects with a grade of 2 or higher. **Table 5** summarizes the sensitivity and specificity of this parameter when measured by OCT and UBM.

Table 1. Distribution of Gonioscopic Grade Classified Using a Modified Shaffer Scale*

Gonioscopic Grade	Eyes, No. (%)
0	5 (16.1)
1	3 (9.7)
2	5 (16.1)
3	7 (22.6)
4	11 (35.5)

*Two subjects classified as grade 1 in the nasal angle were classified as grade 0 (iris/trabecular apposition) in the temporal angle and were considered grade 0. All of the other subjects had symmetric angle grades.

COMMENT

Although gonioscopy has been the clinical standard for characterizing the AC angle, it is a subjective procedure and requires the expertise of a specialized physician. Cross-sectional imaging methods like ultrasound biomicroscopy and Scheimpflug photography[30] have been used to define AC angle characteristics in a more objective manner.

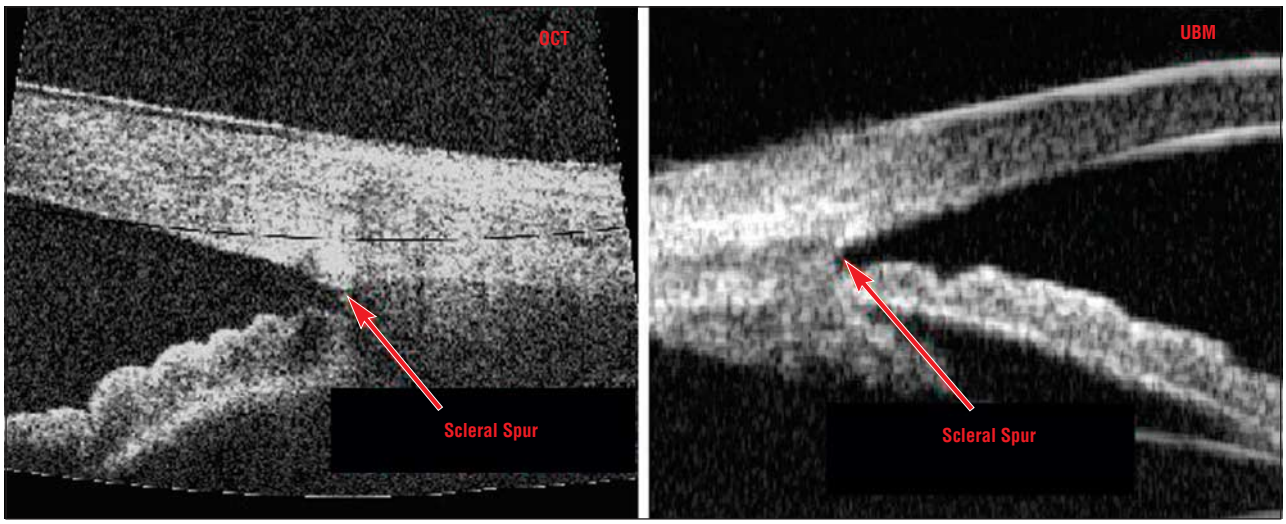

Figure 4. Side-by-side comparison of an optical coherence tomographic (OCT) image and an ultrasound biomicroscopic (UBM) image of the anterior chamber angle obtained from a single subject.

Table 2. Angle Opening Distance, Angle Recess Area, and Trabecular-Iris Space Area Measured by Ultrasound Biomicroscopy and Optical Coherence Tomography (n = 31 Eyes)*

Parameter	UBM, Mean (SD)	OCT, Mean (SD)	*P* Value
Nasal quadrant			
AOD 500, mm	0.37 (0.055)	0.44 (0.056)	.06
ARA 500, mm^2	0.15 (0.028)	0.17 (0.024)	.02
ARA 750, mm^2	0.26 (0.036)	0.29 (0.040)	.03
TISA 500, mm^2	0.15 (0.026)	0.15 (0.018)	.76
TISA 750, mm^2	0.23 (0.027)	0.26 (0.029)	.01
Temporal quadrant			
AOD 500, mm	0.41 (0.072)	0.44 (0.058)	.10
ARA 500, mm^2	0.19 (0.097)	0.18 (0.051)	.88
ARA 750, mm^2	0.29 (0.079)	0.32 (0.077)	.06
TISA 500, mm^2	0.18 (0.091)	0.17 (0.047)	.81
TISA 750, mm^2	0.27 (0.074)	0.30 (0.078)	.07

Abbreviations: AOD 500, angle opening distance at 500 µm; ARA 500, angle recess area at 500 µm; ARA 750, angle recess area at 750 µm; OCT, optical coherence tomography; TISA 500, trabecular-iris space area at 500 µm; TISA 750, trabecular-iris space area at 750 µm; UBM, ultrasound biomicroscopy.

*Standard deviations were pooled from 3 repeated measures for each parameter. None of the differences in repeatability between UBM and OCT were statistically significant.

Table 3. Accuracy of Classification of Subjects With Occludable Angles (Gonioscopic Grade ≤1) by Angle Opening Distance, Angle Recess Area, and Trabecular-Iris Space Area, Each Measured at 500 µm and 750 µm by Ultrasound Biomicroscopy and Optical Coherence Tomography*

Parameter	Sensitivity, %	Specificity, %	Cutoff Value
AOD 500			
UBM	87.5	95.7	200 µm
OCT	100.0	87.5	191 µm
ARA 500			
UBM	91.3	87.5	0.07 mm^2
OCT	87.0	100.0	0.12 mm^2
ARA 750			
UBM	100.0	87.5	0.12 mm^2
OCT	91.3	87.5	0.17 mm^2
TISA 500			
UBM	87.0	87.5	0.08 mm^2
OCT	87.0	100.0	0.11 mm^2
TISA 750			
UBM	90.9	87.5	0.14 mm^2
OCT	91.3	87.5	0.17 mm^2

Abbreviations: AOD 500, angle opening distance at 500 µm; ARA 500, angle recess area at 500 µm; ARA 750, angle recess area at 750 µm; OCT, optical coherence tomography; TISA 500, trabecular-iris space area at 500 µm; TISA 750, trabecular-iris space area at 750 µm; UBM, ultrasound biomicroscopy.

*For each imaging modality, the average value of the 2 measurements from the nasal and temporal quadrants was used for each eye (n = 31 eyes).

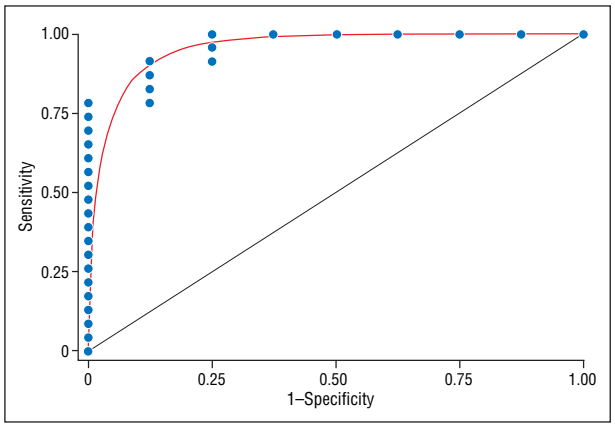

Figure 5. Receiver operating characteristic curve for the trabecular-iris space area at 750 µm. Area under the receiver operating characteristic curve = 0.9559; standard error of area = 0.04.

Ultrasound biomicroscopy provides high-resolution images (50-µm lateral resolution in the commercially available system) of the AC angle region, has a depth of penetration of 5 mm in tissue, and is able to image through opaque media. However, it has several limitations. A coupling medium is required such that scanning must be performed through an immersion bath. The procedure is time-consuming and requires a highly skilled operator to obtain high-quality images. There is a risk of infection or corneal abrasion due to the contact nature of the examination. Finally, inadvertent pressure on the eyecup used while scanning can influence the angle configuration, as demonstrated by Ishikawa et al[31] using a small UBM eyecup.

Scheimpflug photography is another technique that has been used for quantitative evaluation of the AC angle.[32] However, the actual AC angle recess is not visualized by this technique and, thus, important structural information in this region is likely to be missed.

Optical coherence tomography is a light-based imaging modality that has several advantages over the other techniques used for objective assessment of the AC angle. It has a higher image resolution than UBM, is totally noncontact, and is easily performed with minimal expertise. The noncontact nature of OCT not only enhances patient comfort and safety but also makes it especially suitable for ocular biometry and AC angle assessment since there is no mechanical distortion of the tissue being imaged. Unlike 0.8-µm OCT, which is best suited for retinal imaging, 1.3-µm OCT provides excellent visualization of both the cornea and the AC angle, thus broadening the scope of potential applications for this system. Due to the lower scattering loss at 1.3 µm, highly detailed AC angle imaging is possible, and angle structures including the iris root, the angle recess, the anterior ciliary body, the scleral spur, and, in some eyes, the canal of Schlemm can be visualized. Objective assessment of the angle characteristics can also be made from the OCT images.

In this study, we have focused on AC angle imaging with 1.3-µm OCT. We used gonioscopy to define angle status since it is the currently accepted standard for the clinical diagnosis of narrow angles. Using this standard, we evaluated several quantitative AC angle parameters obtained by OCT and UBM for sensitivity and specificity in the detection of narrow angles.

IMAGE QUALITY IN OCT VS UBM

Excellent delineation of angle structures and the iris surface is possible with OCT. Visualization of the ciliary body

Table 4. Area Under the Receiver Operating Characteristic Curve for All Parameters Measured With Ultrasound Biomicroscopy and Optical Coherence Tomography*

Parameter	AUC (95% CI)
AOD 500	
UBM	0.97 (0.92-1.00)
OCT	0.98 (0.95-1.00)
ARA 500	
UBM	0.96 (0.90-1.00)
OCT	0.97 (0.92-1.00)
ARA 750	
UBM	0.97 (0.92-1.00)
OCT	0.96 (0.90-1.00)
TISA 500	
UBM	0.96 (0.89-1.00)
OCT	0.97 (0.92-1.00)
TISA 750	
UBM	0.96 (0.89-1.00)
OCT	0.96 (0.90-1.00)

Abbreviations: AOD 500, angle opening distance at 500 µm; ARA 500, angle recess area at 500 µm; ARA 750, angle recess area at 750 µm; AUC, area under the receiver operating characteristic curve; CI, confidence interval; OCT, optical coherence tomography; TISA 500, trabecular-iris space area at 500 µm; TISA 750, trabecular-iris space area at 750 µm; UBM, ultrasound biomicroscopy.

*Alternative definitions of a positive test result were evaluated for each parameter to identify optimum values that provided the best possible mix of sensitivity and specificity. The average of the 2 measurements from the nasal and temporal quadrants was used for each eye.

with OCT is not as complete as with UBM, and the angle recess may not be well defined in some eyes. However, critical landmarks such as the scleral spur are more distinct in OCT images.

QUANTITATIVE AC ANGLE PARAMETERS IN OCT VS UBM

The reproducibility of OCT was found to be equal to that of UBM. Both OCT and UBM provided similar mean values for various anterior segment parameters. When a statistically significant difference was present, UBM tended to give smaller measurements.

Several factors may account for the difference between OCT and UBM measurements:

1. Differences in instrument calibration: The UBM instrument assumes a speed of sound of 1530 m/s in all tissues,[33] which ignores subtle speed variations that exist in the various ocular tissues. For OCT measurements, we assumed a group index of 1.33 for the aqueous humor to convert optical delay to geometric depth.[34] However, the true refractive index at 1.3 µm may be slightly higher. (A group index of 1.34 was recently measured in eye bank corneas using a 1.3-µm OCT system [R. Lin, BS, written communication, December 1, 2001].) These calibration errors are, however, insignificant when compared with the population variance of angle parameters and do not affect the sensitivity and specificity of detecting narrow angles.

2. Patient position during imaging: Optical coherence tomography was performed in the sitting position whereas UBM imaging was performed in the supine position. Angle measurements may reasonably be expected to be larger in the supine position; however, in our data set, the UBM measurements tended to be smaller than the OCT measurements.

3. Effect of the UBM eyecup: In this study, large-sized UBM eyecups (22-mm and 24-mm) were used, and it is possible that inadvertent posterior pressure on the eyecup may cause artificial narrowing of the angle.

4. Illumination: Although we attempted to standardize the lighting conditions for OCT and UBM imaging, it is possible that small variations in illumination occurred. The resultant small changes in pupil size can cause variations in measurement between the 2 techniques.

5. Variations in the location of the scan: Scanning was performed in the horizontal meridian with both techniques; however, it was not possible to determine the exact location of the scan. Hence, variations from meridian to meridian could have affected the final measurements. Further development of the anterior segment OCT prototype to enable visualization of the scan beam can aid in determining the scan location.

Table 5. Accuracy of Classification of Subjects With Narrow Angles (Gonioscopic Grade ≤1) by Trabecular-Iris Contact Length Measured by Ultrasound Biomicroscopy and Optical Coherence Tomography*

Technique	Sensitivity, %	Specificity, %
UBM	87.5	79.3
OCT	62.5	100.0

Abbreviations: OCT, optical coherence tomography; UBM, ultrasound biomicroscopy.

*The trabecular-iris contact length was considered diagnostic of a narrow angle if any of the 6 images (3 in each of the nasal and temporal quadrants) showed trabecular-iris contact (n = 31 eyes).

DETECTION OF NARROW ANGLES WITH OCT VS UBM

In addition to the AOD and the ARA, which have been described previously in UBM studies, we used 2 new parameters: the TISA and the TICL for defining AC angle anatomy. The TISA differs from the ARA in that it only measures the filtering area in front of the scleral spur whereas the ARA also includes the nonfiltering angle recess. Thus, the ARA may be less sensitive in identifying a narrow angle in eyes with a relatively deep angle recess. In our small data set, we did not encounter patients with these characteristics, and both the ARA and the TISA performed equally well. In OCT imaging, another advantage of the TISA over the ARA is that identification of the scleral spur is more reliable than the angle recess. This is because the scleral spur is highly reflective and appears bright on the OCT image whereas the recess is less reflective and may be less precisely defined in some eyes.

Both OCT and UBM showed excellent discriminative value for the detection of narrow angles. Based on the AUC, the best OCT parameters for detecting narrow angles were the AOD 500, ARA 500, and TISA 500 (AUC ≥0.97). However, the ARA 750 and the TISA 750 also provided excellent discrimination (AUC = 0.96). Theoretically, 500 µm is

the appropriate measurement distance for angle areas because it approximates the length of the trabecular meshwork. However, a longer measurement distance of 750 µm uses information from a large region of the image and may be more robust since it would be less affected by local iris surface undulations. Our current study shows that parameters based on both 500-µm and 750-µm measurement distances were effective for angle assessment.

The TICL as measured by OCT had perfect specificity. This could allow it to be used to aid in narrow angle detection as a combined criterion with the TISA to increase sensitivity without reducing specificity. However, given the excellent performance of the TISA alone, we did not perform this analysis because of the small size of our current data set.

CONCLUSION

In this pilot study, we have demonstrated a novel potential application for OCT at 1.3 µm. Optical coherence tomography as an imaging modality has several characteristics that make it an excellent candidate for large-scale screening for PACG. We have shown that the quantitative angle parameters as measured by OCT have similar mean values, reproducibility, and sensitivity-specificity profiles when compared with measurements obtained by UBM. In our limited data set, these parameters clearly showed high discriminative value in the detection of narrow angles. The ease of image acquisition and the noncontact nature of OCT are highly desirable. Further study with a larger sample size is required to clearly define the utility of OCT parameters in screening for PACG. Further development of the technology is also needed to design a robust system that can be used in fieldwork. In addition, more experience and additional research are needed to better learn how to apply this new technology to clinical decision making. While keeping these considerations in mind, anterior segment OCT shows great promise in improving our ability to detect individuals at risk for the development of PACG.

Submitted for Publication: January 14, 2004; final revision received November 22, 2004; accepted December 6, 2004.

Correspondence: Scott D. Smith, MD, MPH, Division of Ophthalmology, i32, Cole Eye Institute, The Cleveland Clinic Foundation, 9500 Euclid Ave, Cleveland, OH 44195 (smiths@ccf.org).

Funding/Support: This research was supported by grant R21 EB002718 from the National Institutes of Health, Bethesda, Md (Drs Radhakrishnan, Huang, Westphal, Rollins, and Izatt).

REFERENCES

1. Foster PJ, Johnson GJ. Glaucoma in China: how big is the problem? *Br J Ophthalmol*. 2001;85:1277-1282.
2. Dandona L, Dandona R, Mandal P, et al. Angle-closure glaucoma in an urban population in southern India: the Andhra Pradesh eye disease study. *Ophthalmology*. 2000;107:1710-1716.
3. Chew PT, Aung T. Primary angle-closure glaucoma in Asia. *J Glaucoma*. 2001;10: S7-S8.
4. Alsbirk PH. Anterior chamber depth and primary angle-closure glaucoma, I: an epidemiologic study in Greenland Eskimos. *Acta Ophthalmol (Copenh)*. 1975; 53:89-104.
5. Foster PJ, Buhrmann R, Quigley HA, Johnson GJ. The definition and classification of glaucoma in prevalence surveys. *Br J Ophthalmol*. 2002;86:238-242.
6. Friedman DS. Who needs an iridotomy? *Br J Ophthalmol*. 2001;85:1019-1021.
7. Pavlin CJ, Sherar MD, Foster FS. Subsurface ultrasound microscopic imaging of the intact eye. *Ophthalmology*. 1990;97:244-250.
8. Marchini G, Pagliarusco A, Toscano A, Tosi R, Brunelli C, Bonomi L. Ultrasound biomicroscopic and conventional ultrasonographic study of ocular dimensions in primary angle-closure glaucoma. *Ophthalmology*. 1998;105:2091-2098.
9. Pavlin CJ, Sherar MD, Foster FS. Ultrasound biomicroscopy in plateau iris syndrome. *Am J Ophthalmol*. 1992;113:390-395.
10. Sakuma T, Sawada A, Yamamoto T, Kitazawa Y. Appositional angle closure in eyes with narrow angles: an ultrasound biomicroscopic study. *J Glaucoma*. 1997; 6:165-169.
11. Pavlin CJ, Foster FS. Plateau iris syndrome: angle opening changes with dark, light, and pilocarpine. *Am J Ophthalmol*. 1999;128:288-291.
12. Huang D, Swanson EA, Lin CP, et al. Optical coherence tomography. *Science*. 1991;254:1178-1181.
13. Swanson EA, Izatt JA, Hee MR, et al. In vivo retinal imaging by optical coherence tomography. *Opt Lett*. 1993;21:1864-1866.
14. Hee MR, Izatt JA, Swanson EA, et al. Optical coherence tomography of the human retina. *Arch Ophthalmol*. 1995;113:325-332.
15. Izatt JA, Hee MR, Swanson EA, et al. Micrometer-scale resolution imaging of the anterior eye in vivo with optical coherence tomography. *Arch Ophthalmol*. 1994; 112:1584-1589.
16. Hoerauf H, Wirbelauer C, Scholz C, et al. Slit-lamp-adapted optical coherence tomography of the anterior segment. *Graefes Arch Clin Exp Ophthalmol*. 2000; 238:8-18.
17. Maldonado MJ, Ruiz-Oblitas L, Munuera JM, Aliseda D, Garcia-Layana A, Moreno-Montanes J. Optical coherence tomography evaluation of the corneal cap and stromal bed features after laser in situ keratomileusis for high myopia and astigmatism. *Ophthalmology*. 2000;107:81-87.
18. Bechmann M, Thiel MJ, Neubauer AS, et al. Central corneal thickness measurement with a retinal optical coherence tomography device versus standard ultrasonic pachymetry. *Cornea*. 2001;20:50-54.
19. Muscat S, McKay N, Parks S, Kemp E, Keating D. Repeatability and reproducibility of corneal thickness measurements by optical coherence tomography. *Invest Ophthalmol Vis Sci*. 2002;43:1791-1795.
20. Ustundag C, Bahcecioglu H, Ozdamar A, Aras C, Yildirim R, Ozkan S. Optical coherence tomography for evaluation of anatomical changes in the cornea after laser in situ keratomileusis. *J Cataract Refract Surg*. 2000;26:1458-1462.
21. Nozaki M, Kimura H, Kojima M, Ogura Y. Optical coherence tomographic finding of the anterior segment after non-penetrating deep sclerectomy. *Am J Ophthalmol*. 2002;133:837-839.
22. Rollins AM, Izatt JA. Optimal interferometer designs for optical coherence tomography. *Opt Lett*. 1999;24:1484-1486.
23. van den Berg TJTP, Spekreijse H. Near infrared light absorption in the human eye media. *Vision Res*. 1997;37:249-253.
24. Hoerauf H, Gordes RS, Scholz C, et al. First experimental and clinical results with transscleral optical coherence tomography. *Ophthalmic Surg Lasers*. 2000; 31:218-222.
25. Radhakrishnan S, Rollins AM, Roth JE, et al. Real-time optical coherence tomography of the anterior segment at 1310 nm. *Arch Ophthalmol*. 2001;119: 1179-1185.
26. American National Standards Institute. *American National Standard for Safe Use of Lasers, ANSI Z 136.1-2000*. Orlando, Fla: Laser Institute of America; 2000:45-49.
27. Westphal V, Rollins AM, Radhakrishnan S, Izatt JA. Correction of geometric and refractive image distortions in optical coherence tomography applying Fermat's principle. *Opt Express*. 2002;10:397-404.
28. Pavlin CJ, Harasiewicz K, Foster FS. Ultrasound biomicroscopy of anterior segment structures in normal and glaucomatous eyes. *Am J Ophthalmol*. 1992; 113:381-389.
29. Ishikawa H, Liebmann JM, Ritch R. Quantitative assessment of the anterior segment using ultrasound biomicroscopy. *Curr Opin Ophthalmol*. 2000;11:133-139.
30. Dragomirescu V, Hockwin O, Koch H-R, et al. Development of a new equipment for rotating slit image photography according to Scheimpflug's principle. *Interdiscip Top Gerontol*. 1978;13:118-130.
31. Ishikawa H, Inazumi K, Liebmann JM, Ritch R. Inadvertent corneal indentation can cause artifactitious widening of the iridocorneal angle on ultrasound biomicroscopy. *Ophthalmic Surg Lasers*. 2000;31:342-345.
32. Boker T, Sheqem J, Rauwolf M, Wegener A. Anterior chamber angle biometry: a comparison of Scheimpflug photography and ultrasound biomicroscopy. *Ophthalmic Res*. 1995;27(suppl 1):104-109.
33. Pavlin CJ, Foster FS. Examination techniques. In: *Ultrasound Biomicroscopy of the Eye*. New York, NY: Springer Verlag; 1995:45.
34. Maurice DM. The cornea and sclera. In: Davson H, ed. *The Eye*. Vol 1B. 3rd ed. Orlando, Fla: Academic Press; 1984:46.